





Epigenetic and genetic inactivation of tumor suppressor *miR-135a* in non-small-cell lung cancer

Jin Eun Choi¹  | Hyo Sung Jeon¹ | Hyun Jung Wee¹ | Ji Yun Lee¹ |
 Won Kee Lee² | Shin Yup Lee^{3,4}  | Seung Soo Yoo^{3,4}  | Sun Ha Choi^{3,4} |
 Dong Sun Kim^{1,5} | Jae Yong Park^{1,3,4} 

¹Cell and Matrix Research Institute, School of Medicine, Kyungpook National University, Daegu, South Korea

²Biostatistics, Medical Research Collaboration Center in Kyungpook National University Hospital and School of Medicine, Kyungpook National University, Daegu, South Korea

³Department of Internal Medicine, School of Medicine, Kyungpook National University, Daegu, South Korea

⁴Lung Cancer Center, Kyungpook National University Chilgok Hospital, Daegu, South Korea

⁵Department of Anatomy, School of Medicine, Kyungpook National University, Daegu, South Korea

Co-Correspondence

Jae Yong Park, MD, PhD, Lung Cancer Center, Kyungpook National University Medical Center, 807, Hoguk-ro, Buk-gu, Daegu 702-210, Korea; Email: jaeyong@knu.ac.kr

Dong Sun Kim, PhD, Department of Anatomy, School of Medicine, Kyungpook National University, 680 Gukchaebosang-ro, Jung-gu, Daegu 41 944, Republic of Korea; E-mail address: Email: doskim@knu.ac.kr

Abstract

Background: Despite therapeutic advances, lung cancer prognosis remains poor. Loss of heterozygosity (LOH) in the 3p21 region is well documented in lung cancer, but the specific causative genes have not been identified.

Materials and Methods: Here, we aimed to examine the clinical impact of *miR-135a*, located in the 3p21 region, in lung cancer. *miR-135a* expression was assessed using quantitative real-time polymerase chain reaction. LOH was analyzed at microsatellite loci D3S1076 and D3S1478, and promoter methylation status was determined by pyrosequencing of resected samples of primary non-small-cell lung cancer (NSCLC). The regulation of telomerase reverse transcriptase (TERT) was evaluated in lung cancer cells H1299 by luciferase report assays after treatment with *miR-135a* mimics.

Results: *miR-135a* was significantly downregulated in squamous cell cancer (SCC) tumor tissues compared to normal tissues ($p = 0.001$). Low *miR-135a* expression was more frequent in patients with SCC ($p = 2.9 \times 10^{-4}$) and smokers ($p = 0.01$). LOH and hypermethylation were detected in 27.8% (37/133) and 17.3% (23/133) of the tumors, respectively. Overall, 36.8% (49/133) of the NSCLC cases harbored either *miR-135a* LOH or promoter hypermethylation. The frequencies of LOH and hypermethylation were significantly associated with SCCs ($p = 2 \times 10^{-4}$) and late-stage ($p = 0.04$), respectively. *MiR-135a* inhibited the relative luciferase activity of *psi-CHECK2-TERT-3'UTR*.

Conclusion: These results suggest that *miR-135a* may act as a tumor suppressor to play an important role in lung cancer carcinogenesis, which will provide a new insight into the translational value of *miR-135a*. Further large-scale studies are required to confirm these findings.

KEYWORDS

DNA methylation, loss of heterozygosity, methylation prediction region, *miR-135a*, non-small-cell lung cancer

INTRODUCTION

Lung cancer is the most prevalent cancer and a leading cause of cancer-related death worldwide, with non-small-cell lung cancer (NSCLC) accounting for the majority of cases.¹ Patients with NSCLC have a poor overall survival owing to diagnosis at an advanced stage and unsatisfactory

monitoring for recurrence.² In addition, the molecular mechanisms underlying the clinical, pathological, and global variations in NSCLC behavior remain poorly understood.^{3,4} Thus, research studies on suitable biomarkers are needed to improve the treatment and prevention of NSCLC.

MicroRNAs (miRNAs) are endogenous small (~22 nucleotides) noncoding RNAs that regulate gene

expression via complementary binding to the 3'-untranslated region of target mRNAs, thereby repressing translation or decreasing mRNA stability.⁵ Accumulating evidence has indicated that miRNAs play important roles in the proliferation, migration, and invasion of cancer cells.⁶ Emerging data have shown that *miR-135a* is dysregulated in various cancers and regulates tumor-related biological behaviors.⁷ MiR-135a can inhibit the progression of cancer by targeting various mRNAs, leading to the inactivation of several pathways, including the PI3K/AKT, JAK2/STAT3, and NF- κ B pathways.^{8,9} MiR-135a can also promote cancer development via activation of both the Wnt/ β -catenin and STAT3 pathways.^{10,11} Interestingly, recent studies have shown that miR-135a exhibits both pro- and antitumor effects in lung cancer, acting as either oncogenes or tumor suppressors.¹² MiR135a induces apoptosis and inhibits invasion and angiogenesis by targeting IGF-1 and KLF8,^{13,14} whereas it contributes to lung cancer progression by targeting LOXL4 and promoting chemoresistance.^{15,16} Interestingly, the *miR-135a* gene is located in the 3p21 region, which contains numerous tumor suppressor genes and has a high prevalence of loss of heterozygosity (LOH) in patients with lung cancer.^{17,18} Therefore, to ascertain the involvement of miR-135a and established its clinical role in NSCLC pathogenesis, we determined the expression, LOH, and methylation status of the *miR-135a* gene in resected lung tissues of NSCLC patients and investigated their correlation with clinicopathologic features.

METHODS

Patients and genomic DNA isolation

Tumor and corresponding nonmalignant lung tissue specimens ($n = 133$) were procured by the National Biobank of Korea, Kyungpook National University Hospital, a member of the Korea Biobank Network. The specimens were obtained with informed consent following institutional review board approved protocols. All tumor and normal lung tissue samples were obtained at the time of surgery, flash frozen in liquid nitrogen and stored at -80°C until further analysis. Only tumors with $>80\%$ components were sent for nucleotide extraction and analysis. Normal lung tissues were macroscopically confirmed to be normal by hematoxylin-eosin staining. Genomic DNA was extracted using a QIAamp DNA Mini kit (Qiagen Inc.) according to the manufacturer's instructions.

LOH analysis

Two microsatellite markers (D3S1076 and D3S1478) were used to search for LOH on chromosomes 3p21.1–3p21.3.

The PCR primers and conditions for these markers have been previously described.^{19,20} Fluorescein-labeled PCR products were electrophoresed on an ABI 3130XL DNA sequencer (PE Applied Biosystems). Each allele was scored by comparing the ratio of the peak heights between the tumor (T) and the corresponding normal (N) samples in heterozygous alleles. Based on the formula $T_1:T_2/N_1:N_2$, where 1 stands for the higher and 2 stands for the lower peak height, LOH was defined when the ratio values were <0.5 or >2 . All samples showing LOH result were confirmed as least twice.

Prediction of the miR-135a promoter region

Two candidate promoter regions were predicted by searching two public databases. First, we predicted the *miR-135a* promoter region (-4523 to -4859 relative to the *miR-135a* coding start site) using the UCSC Genomics Browser (<https://genome.ucsc.edu/index.html>), and termed as a promoter-like signature (PLS) region.²¹ However, CpG islands (CGIs) were not predicted in this region. Subsequently, using the online sliding window algorithm CpGPlot in the EMBOSS package,²² we found a CGI spanning nucleotides $-23\ 526$ to $-24\ 115$ following the deposition of 50 000 bp prior to the 5' end of pre-*miR-135a*. We termed this the methylation prediction region (MPR).

Cell culture and 5-aza-2'-deoxycytidine treatment

NSCLC cell lines A549, H1299, H520, and H157 were purchased from the Korean Cell Line Bank and maintained in Corning[®] RPMI medium (Corning Inc.). The cells were cultured in media supplemented with 10% FBS (Corning) and antibiotics in a humidity-controlled environment (37°C , 5% CO_2). A549 and H1299 cells were treated with 10 or 20 μM 5-aza-2'-deoxycytidine (5-AdC) for 3 days and the culture medium was changed daily.

Plasmid construct, transfection, and luciferase assay

Two candidate *miR-135a* promoter regions (PLS and MPR) and the *TERT* 3'-UTR fragment were PCR-amplified from human genomic DNA and cloned into the pGL3-basic and psiCHECK2 vectors (Promega), respectively. All cloned constructs were sequenced to ensure sequence identity and the used primers sequence is given in Supporting Information Table S1. PLS- and MPR-harboring plasmids and pRL-SV40 (Promega) were transiently transfected into cultured cells with 80–90% confluence using Lipofectamine 2000 (Thermo Fisher

Scientific) according to the manufacturer's instructions. The *TERT* 3'-UTR construct was also co-transfected into grown cells with scramble miRNA or *miR-135a-5p* mimics. Luciferase activity was analyzed using the Dual-Luciferase Reporter Assay System (Promega) 48 h post-transfection, according to the manufacturer's protocol. The relative luciferase activity was determined by the ratio of *Renilla* luciferase substrate fluorescence to firefly luciferase substrate fluorescence. The data are shown as the mean \pm SD of three independent experiments.

DNA bisulfite treatment and pyrosequencing

Genomic DNA was chemically modified using a EZ DNA Methylation-Gold kit (Zymo Research) according to the manufacturer's protocol. The methylation status of *miR-135a* MPR (−23 675 to −23 876 bp) was quantitatively determined by pyrosequencing. Briefly, bisulfite-modified DNA was amplified using forward primer 5'-GGGTAGGTAAGGGTTTAGGT-3' and reverse primer biotin-5'-CAAACCTCTAAAAACCCCATTC-3'. The PCR product quality was confirmed by electrophoresing on 2% agarose gels stained with ethidium bromide. After purification of the PCR product with Sepharose beads on a PyroMark Vacuum Prep Workstation (Qiagen), pyrosequencing was performed according to the manufacturer's specifications using a sequencing primer (5'-GGTAAGGGTTTAGGTTG-3') and PyroMark Q96MD System (Qiagen). The average methylation index (MI) was calculated from the mean methylation percentage of the nine evaluated CpG sites. To set the controls for pyrosequencing, CpGenome™ Universal methylated and unmethylated DNA (Chemicon) with stable levels of methylation was used as positive and negative controls, respectively. Each pyrosequencing was repeated at least twice to confirm the results.

RNA extraction and quantitative RT-PCR

Total RNA was isolated from frozen tissues and cells using TRIzol® (Invitrogen). To measure *miR-135a* miRNA and U6 snRNA expression, cDNA was synthesized from 10 ng of total RNA using specific miRNA primers (TaqMan MicroRNA Assay, PN 4427975; PE Applied Biosystems) and a TaqMan MicroRNA Reverse Transcription Kit (PN 4366596; PE Applied Biosystems). Two microliters of cDNA was used as a template in 10 μ l of PCR mixture. PCR target regions were amplified using specific primers (TaqMan MicroRNA Assay) with TaqMan Universal PCR Master Mix II (PN 4440040; PE Applied Biosystems) and detected using a LightCycler 480. The relative *miR-135a* miRNA expression was normalized to U6 snRNA expression, and the data were analyzed using the $2^{-\Delta\Delta C_t}$ method.

Statistical analysis

Student's *t*-test was used for the comparison of continuous variables, and the chi-square test or Fisher's exact test was used for comparison of categorical variables. All analyses were conducted using the Statistical Analysis System for Windows, version 9.1 (SAS Institute), and graphical representations were constructed using the ggplot2 package of the R program and Microsoft Excel 2019 (Microsoft).

RESULTS

Expression of miR-135a mRNA and its correlation with clinicopathological characteristics in patients with NSCLC

We measured the expression levels of *miR-135a* in 80 tumors and their corresponding normal lung tissues using quantitative real-time polymerase chain reaction (RT-PCR). We observed that tumor tissues with squamous cell carcinomas (SCCs) exhibited significantly decreased *miR-135a* mRNA expression ($p = 0.001$) compared to normal tissues (Figure 1). However, there was no significant decrease in *miR-135a* expression between tumor and normal tissues in all patients or in adenocarcinomas (ADCs). Furthermore, we analyzed the correlation between *miR-135a* expression and the clinicopathological features of NSCLC patients. The patients with NSCLC were classified into *miR-135a* high- and low-expression groups based on the median level. There was a significant association between low expression of *miR-135a* and SCC ($p = 2.9 \times 10^{-4}$) and smokers ($p = 0.01$). However, no significant difference in *miR-135a* expression was found according to age, gender, and pathologic stage (Table 1).

Promoter assay of PLS and MPR regions of miR-135a and 5-AzadC effect on miR-135a expression

We selected two *miR-135a* candidate promoter regions (PLS and MPR) identified using UCSC genome browsers. To address whether these regions exhibited promoter activity, we generated two predicted pGL3-miR-135a promoter constructs using pGL3-basic, pGL3-miR-135a-PLS (−4523 to −4859) and pGL3-miR-135a-MPR (−23 526 to −24 115) (Figure 2a), and transfected them into A549 and H1299 cells. There was no significant difference in luciferase activity between the pGL3-basic and pGL3-miR-135a-PLS plasmids, whereas the luciferase activity was remarkably higher in A549 and H1299 cells harboring the pGL3-miR-135a-MPR construct than those harboring pGL3-miR-135a-PLS (Figure 2b). These results suggest that the MPR might be a putative promoter region that regulates *miR-135a* expression.

Next, to elucidate whether promoter methylation was involved in regulating *miR-135a* expression, we investigated MPR methylation status and *miR-135a* expression level in four lung cancer cell lines (Figure 3a). *MiR-135a* expression was relatively low in A549, H157, and H1299 cells, which harbored methylated MPR, whereas H520 cells harboring unmethylated MPR showed high expression of *miR-135a* mRNA. Furthermore, we treated H1299 and A549 cells with the demethylating agent 5-AdC, which restored *miR-135a* expression in a dose-dependent manner (Figure 3b). Collectively, these results suggest that the methylation status of the MPR region could regulate the *miR-135a* expression.

Hypermethylation and LOH of the *miR-135a* gene in NSCLCs and correlation with clinicopathological factors

We determined the methylation status of the MPR region of the *miR-135a* gene in the primary lung tumor tissues of 133 NSCLC patients using pyrosequencing. The pyrosequencing primers were designed to encompass nine CpGs from 23 581 to 23 636 bp upstream of the transcription start site. Accurate and reproducible estimates of methylated cytosine content were obtained for all the tested samples, and representative pyrograms are shown in Figure 4. Pyrosequencing of representative PCR products showed that all cytosines at non-CpG sites were converted to thymines, ruling out the possibility of incomplete bisulfite conversion. Considering a mean methylation index (9.95%) for all nonmalignant lung tissues, we set 19.9 (>2-fold) as the cut-off point for “hypermethylation” classification. *MiR-135a* was hypermethylated in the tumor tissue compared with matching normal tissue (54N vs. 54T), whereas obvious hypermethylation was undetectable in another tumor tissue (25N vs. 25T) (Figure 4). *MiR-135a* hypermethylation was detected exclusively in malignant tissues at a frequency of 17.3% (23/133) (Table 2), suggesting that *miR-135a* hypermethylation may be a tumor-associated event in NSCLC tumorigenesis.

Furthermore, hypermethylation was more frequent in late-stage NSCLCs ($p = 0.04$). These results represent the first demonstration of aberrant methylation of *miR-135a* in the primary tumors of patients with NSCLC.

We tested the LOH of the *miR-135a* locus in primary tumor tissues using the D3S1076 and D3S1478 microsatellite markers because *miR-135a* is a putative tumor suppressor gene located in the 3p21 region. LOH was detected in 37 (27.8%) of the 133 tumor specimens; 10 tumor samples showed LOH at both markers and 27 showed LOH at one marker (Table 2). In total, 36.8% (49/133) of the NSCLCs harbored *miR-135a* LOH or hypermethylation. Eleven of the 49 tumors exhibited simultaneous alterations in the same tissues (Table 2). Interestingly, LOH of *miR-135a* was more

TABLE 1 Correlation between *miR-135a* expression levels and the clinicopathological features of Patients with NSCLCs

Features	Number of patients	Low (%)	High (%)	<i>p</i>
All subjects	80	40 (50.0)	40 (50.0)	
Age (years)				
≤63	45	21 (46.7)	24 (53.3)	0.50
>63	35	19 (54.3)	16 (45.7)	
Gender				
Male	60	33 (55.0)	27 (45.0)	0.12
Female	20	7 (35.0)	13 (65.0)	
Smoking status				
Ever	60	5 (25.0)	15 (75.0)	0.01
Never	20	35 (58.3)	25 (41.7)	
Histologic types				
SCC	38	28 (73.7)	10 (26.3)	2.9×10^{-4}
ADC	42	12 (28.6)	30 (71.4)	
Pathologic stages				
Stage I	69	35 (50.7)	34 (49.3)	0.75
Stage II–III	11	5 (45.5)	6 (54.5)	

Abbreviations: SCC, squamous cell carcinoma; ADC, adenocarcinoma.

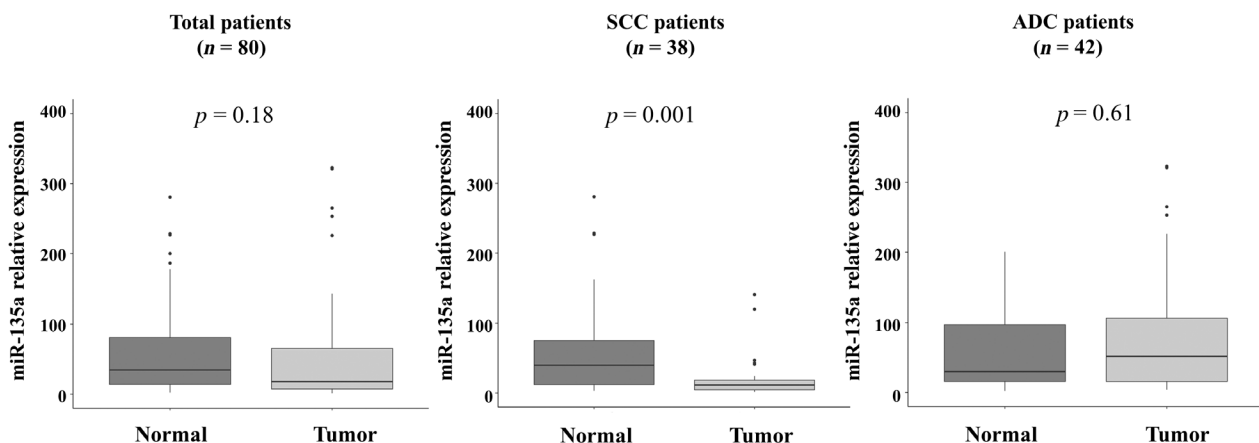


FIGURE 1 *miR-135a* expression in normal and tumor tissues of patients with non-small-cell lung cancer. The *miR-135a* expression level was normalized with that of β -actin gene in 80 patients. *p* values by the paired *t*-test. SCC, squamous cell carcinoma; ADC, adenocarcinoma

frequent in SCCs than in ADCs (41.7% vs. 11.5%, $p = 2 \times 10^{-4}$; Table 2). However, neither LOH nor promoter hypermethylation of *miR-135a* were significantly correlated with overall survival of the patients (data not shown).

Regulation of TERT expression by miR-135a

We identified the potential target genes of miR-135a using MirWalk3.0 (<http://mirwalk.umm.uni-heidelberg.de/>), a miRNA-target prediction tool. Bioinformatics analysis revealed that the 3'-untranslated region (3'-UTR) of

telomerase reverse transcriptase (TERT) contains four direct target sites for *miR-135a-5p* at 3498–4001 bp. To test whether *miR-135a-5p* can specifically regulate *TERT* expression through 3'-UTR, we constructed a dual-luciferase reporter vector psiCHECK2-*TERT* 3'UTR (Figure 5a) and co-transfected into lung cancer cell line H1299 with *miR-135a* mimics or scrambled miRNAs. The relative luciferase activity was significantly decreased in the *miR-135a-5p* mimics group in a dose-dependent manner compared to the scrambled group ($p < 0.05$) (Figure 5b). These results indicate that TERT might be the target gene of *miR-135a-5p*, which may negatively regulate the TERT gene in NSCLC cell lines.

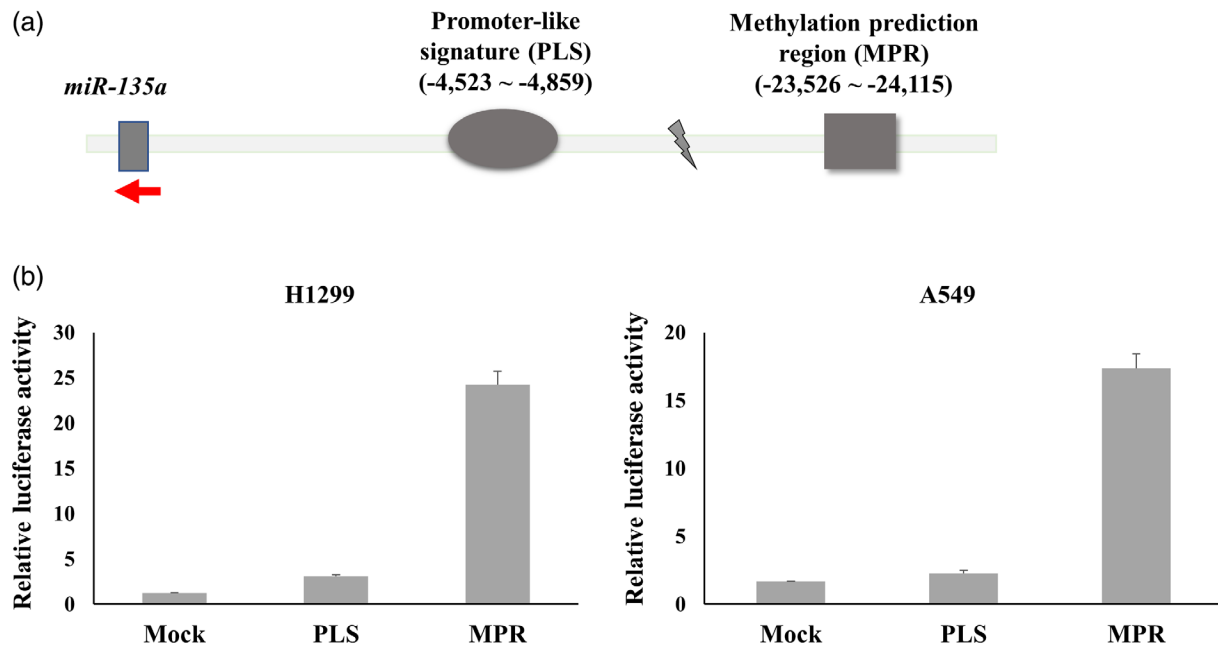


FIGURE 2 Transcriptional activity of putative promoter regions of the *miR-135a* gene. (a) Schematic map of the PLS and MPR of the *miR-135a* gene. (b) Transient luciferase assay detection. H1299 and A549 cell lines were transfected with pGL3-Basic-PLS, pGL3-Basic-MPR constructs, and pRL-SV40 vector (mock). The relative luciferase activity was measured using the Dual-Luciferase Reporter System 48 h post-transfection. All experiments were performed twice in triplicate.

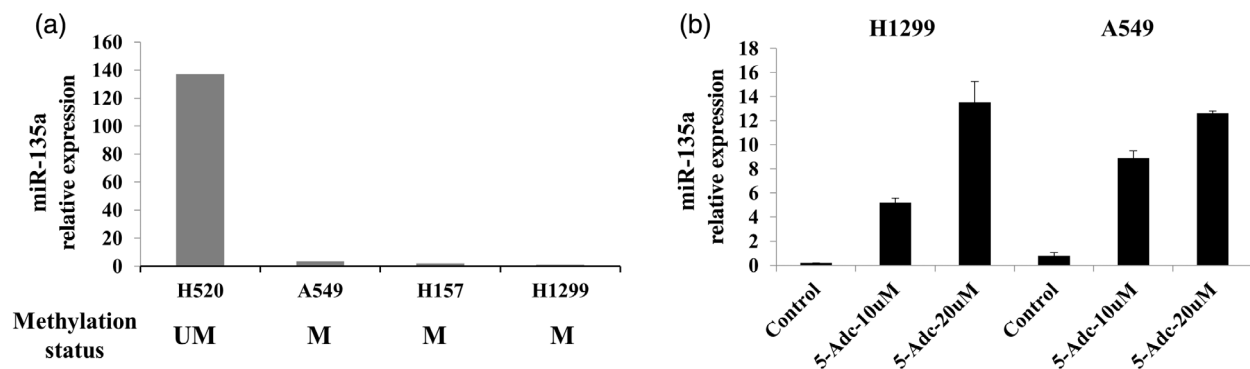


FIGURE 3 Effect of 5-aza-2'-deoxycytidine (5-AdC) on *miR-135a* expression in non-small-cell lung cancer (NSCLC) cell lines. (a) Differential expression of *miR-135a* according to MPR methylation status in four NSCLC cell lines. The *miR-135a* expression level was normalized to that of β -actin. (b) Expression of *miR-135a* mRNA was measured in A549 and H1299 cells following treatment with the demethylation agent 5-AdC for 3 days. UM, unmethylation; M, methylation.

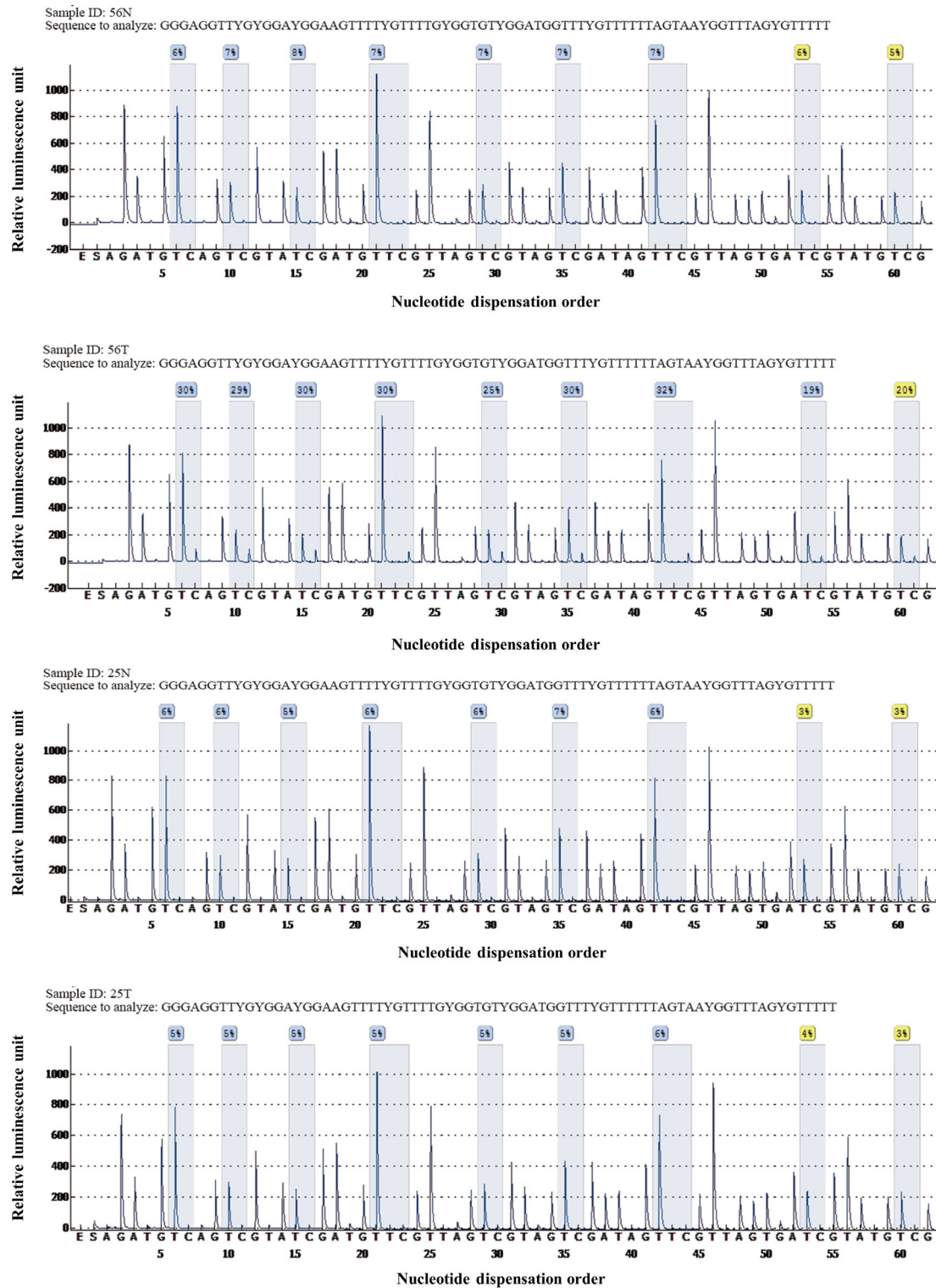


FIGURE 4 Representative pyrograms of the *miR-135a* gene in non-small-cell lung cancer patients. The letters on the axis represent the dispensation order. E, enzyme mix; S, substrate; A, G, C, and T, nucleotides. Shaded bars encompassing T/C pairs indicate eight interrogated CpGs. The methylation of each CpG site was calculated as a percentage of C incorporation. N, normal tissue; T, tumor tissue.

DISCUSSION

Dysregulation of miRNAs has been increasingly recognized as a critical mediator of cancer development and

progression. MiR-135a is a critical regulator of gene expression that targets mRNAs with complementary sequences to suppress their expression. Importantly, it plays important but contradictory roles in cancer progression by acting as

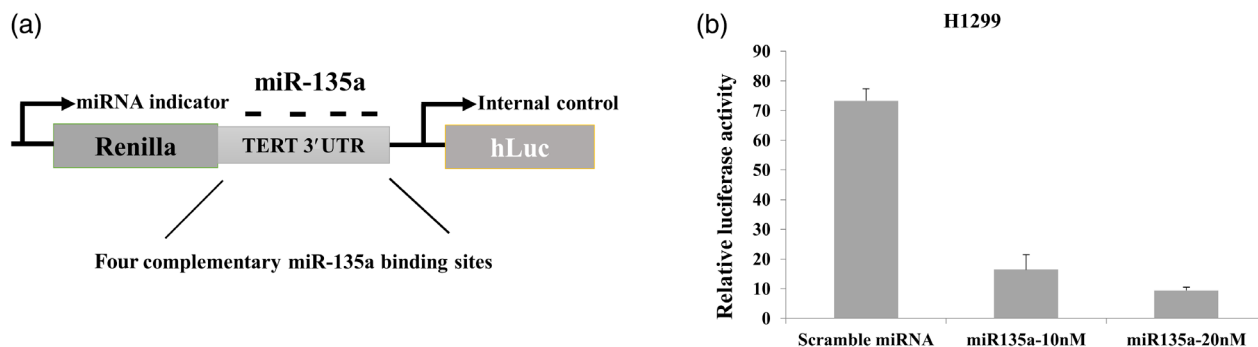


FIGURE 5 Regulation of *TERT* expression by *miR-135a*. (a) The schematic representation of the psiCHECK2-*TERT* 3'UTR construct. (b) H1299 cells were co-transfected with psiCHECK2-*TERT* 3'UTR plasmid and scrambled miRNA or 10 or 20 nM *miR-135a* mimics. Luc was used as the internal control.

TABLE 2 Correlation between LOH and methylation of the *miR-135a* gene and the clinicopathological features of NSCLCs

Feature	LOH (%)	Methylation (%)	LOH or methylation (%)
All subjects ($n = 133$)	37 (27.8)	23 (17.3)	49 (36.8)
Age (years)			
< 64 ($n = 67$)	17 (25.4)	12 (17.9)	24 (35.8)
≥ 64 ($n = 66$)	20 (30.3)	11 (16.7)	25 (37.9)
Gender			
Male ($n = 105$)	31 (29.5)	19 (18.1)	40 (38.1)
Female ($n = 28$)	6 (21.4)	4 (14.3)	9 (32.1)
Smoking status			
Ever ($n = 107$)	32 (29.9)	21 (19.6)	42 (39.3)
Never ($n = 26$)	5 (19.2)	2 (7.7)	7 (26.9)
Histologic types			
SCC ($n = 72$)	30 (41.7) ^a	16 (22.2)	36 (50.0) ^b
ADC ($n = 61$)	7 (11.5)	7 (11.5)	13 (21.3)
Pathologic stages			
Stage I ($n = 72$)	21 (29.2)	8 (11.1)	25 (34.7)
Stage II–IV ($n = 61$)	16 (26.2)	15 (24.6) ^c	24 (39.3)

^a $p = 2 \times 10^{-4}$.

^b $p = 1 \times 10^{-3}$.

^c $p = 0.04$.

either oncogenes or tumor suppressors.⁷ Here, we showed that *miR-135a* expression was significantly decreased in SCC tumor tissues, that LOH or hypermethylation was associated with SCC, and that *TERT* was a downstream target gene of *miR-135a*, suggesting a tumor suppressor role of *miR-135a* and its involvement in a subset of NSCLCs pathogenesis.

The second novel finding of this study is the demonstration of the presence of MPR and its hypermethylation in NSCLC that downregulates *miR-135a* expression. Despite extensive research on the functions of *miR-135a* in various biological processes, little information is available on its transcriptional activation mechanisms. Recent studies have demonstrated that the promoter region located 5 kbp

upstream of the human *miR-135a* stem loop contributes to tamoxifen-mediated breast cancer suppression and that two predicted binding sites for STAT5a within the core promoter region (−1128 to −556 bp to the 5' end of pre-*miR-135a-1*) regulate mouse *miR-135a* promoter activity,^{23,24} thereby suggesting the possibility of the presence of a long-range effective promoter. Interestingly, the genomic distances between the pri-miRNA transcription start sites and pre-miRNA sequences are highly variable.^{25,26} *MiR-135a* is an intragenic miRNA that is generally transcribed with its co-host gene. However, accumulating evidence has shown that intragenic miR genes may also have their own independent TSS.²⁷ Additionally, over 100 miRs are epigenetically regulated in different cancers and the methylation frequency of human miR genes appears to be much higher than that of protein coding genes.²⁸ Accordingly, miR genes are frequently present not only in cancer-associated genomic regions, but also in CGIs.^{29,30} In this regard, we predicted two potential promoter regions of *miR-135a* (−4523 to −4859 and −23 526 to −24 115, PLS and MPR, respectively) using open public databases. We found that the MPR displayed approximately four or five times stronger promoter activity than PLS in NSCLC cell lines, that MPR hypermethylation suppressed *miR-135a* expression, and that 5-AzaC treatment restored *miR-135a* expression in a dose-dependent manner. Interestingly, we observed the opposite feature of two SCC cell lines (H157 vs. H520). Because one fifth of the SCC patients exhibited *miR-135a* methylation (Table 2), even with the same cell type, their methylation pattern could be quite different. Our findings therefore suggest that the MPR may be a potential long-range promoter of *miR-135a* whose activity can be regulated by DNA methylation.

TERT, a catalytic subunit of telomerase, plays a key role in cancer formation, ensuring chromosomal stability by maintaining telomere length and allowing cells to avert senescence.³¹ Using the miRWalk database providing predicted information on miRNA-target interaction,³² we found many possible genes targeted by *miR-135a-5p*. Oshimura et al. have previously shown that suppression of telomerase activity is associated with the introduction

of chromosome 3 into renal cell carcinoma and a putative telomerase repressor gene is mapped to the chromosome 3p14.2-p21.1 region.^{33,34} Recently, human chromosome 3p21.3 has been found to carry *TERT* transcriptional regulators in pancreatic cancer.³⁵ Interestingly, our LOH markers (D3S1076 and D3S1478) overlapped these regions for telomerase repressor function. Taken together, we selected the *TERT* genes as a putative *miR-135a-5p*-targeting gene. Although variable miRNAs are also known as regulators of *TERT* through 3'-UTR binding in many types of cancer,³⁶ until now no miRNAs have been reported to target *TERT* in lung cancer. Thus, the present study is the first report to show that *miR-135a-5p* negatively regulates *TERT* in NSCLC cell lines. Considering the oncogenic role of *TERT*, *miR-135a-5p* targeting *TERT* mRNA may function as tumor suppressor miRNAs and act as telomerase inhibitors in clinical applications. A combination of suppressor miRNAs with available chemotherapy drugs is an approach that has garnered a great deal of interest.³⁷ Lastly, we analyzed the correlation between expression of the *miR-135a-5p* and telomere length, utilizing miRNA expression and telomere length data in the Cancer Genome Atlas (TCGA). Unfortunately, *miR-135a-5p* mature form was not correlated with telomere length (data not shown). This result suggests that telomere length may not be influenced by the *miR-135a-5p* expression and other molecular pathways can affect telomere length in lung cancer. The molecular mechanism underlying the correlation of differential *miR-135a-5p* expression with clinical outcomes should be further explored.

The present study had several limitations. First, *MIR135A1* and *MIR135A2* genes that encode *miR-135a* are located in the human chromosome 3p21.2 and 12q23.1 regions, respectively.⁷ It is unknown in which region the mature *miR-135a* form was expressed. However, no genetic and epigenetic alterations related to lung cancer have been reported in the stem loop lesions of *has-miR-135a* on chromosome 12q23 region. With current technology, it is unknown whether mature *miR-135a-5p* originated from chr3 or chr12. We therefore focused our research on the chromosome 3p21 region. This is a limitation of our study and future research on the promoter of *miR-135a* present in the chr12 region is needed. Second, the retrospective design and small number of samples could introduce potential selection bias in the interpretation of results. Also, the subgroup analysis according to tumor histology and pathologic stage might have a type II error. Third, there was a lack of in vitro functional analysis of *miR-135a* downregulation in lung cancer cells. Nevertheless, this is the first report to demonstrate biallelic inactivation of the *miR-135a* gene in NSCLC, suggesting that tumor suppressor *miR-135a* may contribute the epigenetic and genetic susceptibility to lung cancer.

The present study showed that *miR-135a* expression was significantly decreased in SCC tumor tissues, and that LOH or hypermethylation was associated with SCC. In addition,

our results showed the methylation-mediated suppression of *miR-135a* and the prevalence of genetic and epigenetic alterations of the *miR135a* gene in NSCLC patients. This could provide a new way of thinking about the pathogenic mechanisms of NSCLC. However, further large-scale studies are required to confirm the clinical significance of these findings.

AUTHOR CONTRIBUTIONS

J.E.C. performed the experiments, analyzed the data, and prepared the original draft. D.S.K. and J.Y.P. designed the study and supervised the experiment. H.S.J., H.J.W., and J.Y.L. performed the experiments and analyzed the data. W.K.L. performed the statistical analyses. S.Y.L., S.H.C., and S.S.Y. collected and curated the clinical data and samples. All authors have approved the final manuscript.



ACKNOWLEDGMENTS

This research was supported by the Basic Science Research Program through the National Research Foundation of Korea (NRF) funded by the Ministry of Education, Science and Technology (NRF-2020R111A3067217 and NRF-2020R1A2C1011917).

DISCLOSURE

The authors declare that they have no conflict of interests.

ORCID

Jin Eun Choi  <https://orcid.org/0000-0001-7833-2257>
 Shin Yup Lee  <https://orcid.org/0000-0002-2121-7335>
 Seung Soo Yoo  <https://orcid.org/0000-0002-7309-9254>
 Jae Yong Park  <https://orcid.org/0000-0001-7993-4495>

REFERENCES

1. Siegel RL, Miller KD, Fuchs HE, Jemal A. Cancer statistics. *CA Cancer J Clin.* 2021;71:7–33.
2. Yang CY, Yang JCH, Yang PC. Precision management of advanced non-small cell lung cancer. *Annu Rev Med.* 2020;71:117–36.
3. Yano T, Haro A, Shikada Y, Maruyama R, Maehara Y. Non-small cell lung cancer in never smokers as a representative 'non-smoking-associated lung cancer': epidemiology and clinical features. *Int J Clin Oncol.* 2011;16:287–93.
4. McIntyre A, Ganti AK. Lung cancer – a global perspective. *J Surg Oncol.* 2017;2017(115):550–4.
5. Valencia-Sanchez MA, Liu J, Hannon GJ, Parker R. Control of translation and mRNA degradation by miRNAs and siRNAs. *Genes Dev.* 2006;20:515–24.
6. Esquela-Kerscher A, Slack FJ. Oncomirs – microRNAs with a role in cancer. *Nat Rev Cancer.* 2006;6:259–69.
7. Cao Z, Qiu J, Yang G, Liu Y, Luo W, You L, et al. *MiR-135a* biogenesis and regulation in malignancy: a new hope for cancer research and therapy. *Cancer Biol Med.* 2020;17:569–82.
8. Zhou W, Bi X, Gao G, Sun L. *miRNA-133b* and *miRNA-135a* induce apoptosis via the JAK2/STAT3 signaling pathway in human renal carcinoma cells. *Biomed Pharmacother.* 2016;84:722–9.
9. Xie Y, Li F, Li Z, Shi Z. *MiR-135a* suppresses migration of gastric cancer cells by targeting TRAF5-mediated NF-kappaB activation. *Oncotargets Ther.* 2019;12:975–84.
10. Mao XW, Xiao JQ, Li ZY, Zheng YC, Zhang N. Effects of *miR-135a* on the epithelial-mesenchymal transition, migration and invasion of bladder cancer cells by targeting GSK3beta through the Wnt/beta-catenin signaling pathway. *Exp Mol Med.* 2018;50:e429.

11. Van Renne N, Roca Suarez AA, Duong FHT, Gondeau C, Calabrese D, Fontaine N, et al. MiR-135a-5p-mediated downregulation of protein tyrosine phosphatase receptor delta is a candidate driver of HCV-associated hepatocarcinogenesis. *Gut*. 2018;67:953–62.
12. Garzon R, Calin GA, Croce CM. MicroRNAs in cancer. *Annu Rev Med*. 2009;60:167–79.
13. Zhou Y, Li S, Li J, Wang D, Li Q. Effect of microRNA-135a on cell proliferation, migration, invasion, apoptosis and tumor angiogenesis through the IGF-1/PI3K/Akt signaling pathway in non-small cell lung cancer. *Cell Physiol Biochem*. 2017;42:1431–46.
14. Shi H, Ji Y, Zhang D, Liu Y, Fang P. MiR-135a inhibits migration and invasion and regulates EMT-related marker genes by targeting KLF8 in lung cancer cells. *Biochem Biophys Res Commun*. 2015;465:125–30.
15. Zhang Y, Jiang WL, Yang JY, Huang J, Kang G, Hu HB, et al. Down-regulation of lysyl oxidase-like 4 LOXL4 by miR-135a-5p promotes lung cancer progression in vitro and in vivo. *J Cell Physiol*. 2019;234:18679–87.
16. Zhang T, Wang N. miR-135a confers resistance to gefitinib in non-small cell lung cancer cells by upregulation of RAC1. *Oncol Res*. 2018;26:1191–200.
17. Braga E, Senchenko V, Bazov I, Loginov W, Liu J, Ermilova V, et al. Critical tumor-suppressor gene regions on chromosome 3P in major human epithelial malignancies: allelotyping and quantitative real-time PCR. *Int J Cancer*. 2002;100:534–41.
18. Hirao T, Nelson HH, Ashok TD, Wain JC, Mark EJ, Christiani DC, et al. Tobacco smoke-induced DNA damage and an early age of smoking initiation induce chromosome loss at 3p21 in lung cancer. *Cancer Res*. 2001;61:612–5.
19. Chung T, Cheung TH, Lo WK, Yu MY, Hampton GM, Wong HK, et al. Loss of heterozygosity at the short arm of chromosome 3 in microdissected cervical intraepithelial neoplasia. *Cancer Lett*. 2000;154:189–94.
20. Kanjanavirojkul N, Limpaboon T, Patarapadungkit N, Yuenyao P, Pairojkul C. Chromosome 3p alterations in northeastern Thai women with cervical carcinoma. *Asian Pac J Cancer Prev*. 2005;6:501–4.
21. Navarro Gonzalez J, Zweig AS, Speir ML, Schmelter D, Rosenbloom KR, Raney BJ, et al. The UCSC genome browser database: 2021 update. *Nucleic Acids Res*. 2021;49:D1046–57.
22. Rice P, Longden I, Bleasby A. EMBOSS: the European molecular biology open software suite. *Trends Genet*. 2000;16:276–7.
23. Zhang W, Wu M, Chong QY, Zhang M, Zhang X, Hu L, et al. Loss of estrogen-regulated MIR135A1 at 3p21. 1 promotes tamoxifen resistance in breast cancer. *Cancer Res*. 2018;78:4915–28.
24. Wei X, Cheng X, Peng Y, Zheng R, Chai J, Jiang S. STAT5a promotes the transcription of mature mmu-miR-135a in 3T3-L1 cells by binding to both miR-135a-1 and miR-135a-2 promoter elements. *Int J Biochem Cell Biol*. 2016;77:109–19.
25. Georgakilas G, Vlachos IS, Paraskevopoulou MD, Yang P, Zhang Y, Economides AN, et al. microTSS: accurate microRNA transcription start site identification reveals a significant number of divergent pri-miRNAs. *Nat Commun*. 2014;5:1–11.
26. Gao Y, Feng C, Zhang Y, Song C, Chen J, Li Y, et al. TRmir: a comprehensive resource for human transcriptional regulatory information of MiRNAs. *Front Genet*. 2022;13:1–12.
27. Ramalingam P, Palanichamy JK, Singh A, Das P, Bhagat M, Kassab MA, et al. Biogenesis of intronic miRNAs located in clusters by independent transcription and alternative splicing. *RNA*. 2014;20:76–87.
28. Kunej T, Godnic I, Ferdin J, Horvat S, Dovc P, Calin GA. Epigenetic regulation of microRNAs in cancer: an integrated review of literature. *Mutat Res*. 2011;717:77–84.
29. Calin GA, Sevignani C, Dumitru CD, Hyslop T, Noch E, Yendamuri S, et al. Human microRNA genes are frequently located at fragile sites and genomic regions involved in cancers. *Proc Natl Acad Sci USA*. 2004;101:2999–3004.
30. Morales S, Monzo M, Navarro A. Epigenetic regulation mechanisms of microRNA expression. *Biomol Concepts*. 2017;8:203–12.
31. Dratwa M, Wyszczkańska B, Łacina P, Kubik T, Bogunia-Kubik K. TERT-regulation and roles in cancer formation. *Front Immunol*. 2020;11:589929–45.
32. Dweep H, Sticht C, Pandey P, Gretz N. miRWalk-database: prediction of possible miRNA binding sites by walking genes of three genomes. *J Biomed Inform*. 2011;44:839–47.
33. Ohmura H, Tahara H, Suzuki M, Ide T, Shimizu M, Yoshida MA, et al. Restoration of the cellular senescence program and repression of telomerase by human chromosome 3. *Jpn J Cancer Res*. 1995;86:899–904.
34. Tanaka H, Shimizu M, Horikawa I, Kugoh H, Yokata J, Barrett JC, et al. Evidence for a putative telomerase repressor gene in the 3p14.2p21.1 region. *Genes Chromosomes Cancer*. 1998;23:123–33.
35. Yagy T, Ohira T, Shimizu R, Morimoto M, Murakami Y, Hanaki T, et al. Human chromosome 3p21.3 carries TERT transcriptional regulators in pancreatic cancer. *Sci Rep*. 2021;11:15355.
36. Leão R, Apolónio JD, Lee D, Figueiredo A, Tabori U, Castelo-Branco P. Mechanisms of human telomerase reverse transcriptase (hTERT) regulation: clinical impacts in cancer. *J Biomed Sci*. 2018;25:22–34.
37. Reda El Sayed S, Cristante J, Guyon L, Denis J, Chabre O, Cherradi N. MicroRNA therapeutics in cancer: current advances and challenges. *Cancers (Basel)*. 2021;13:2680–708.

SUPPORTING INFORMATION

Additional supporting information can be found online in the Supporting Information section at the end of this article.

How to cite this article: Choi JE, Jeon HS, Wee HJ, Lee JY, Lee WK, Lee SY, et al. Epigenetic and genetic inactivation of tumor suppressor *miR-135a* in non-small-cell lung cancer. *Thorac Cancer*. 2023; 14(11):1012–20. <https://doi.org/10.1111/1759-7714.14838>